Assessment of the multifunctional behavior of lupin peptide P7 and its metabolite using an integrate strategy

Lammi Carmen[1]*, Aiello Gilda[1], Dellafiora Luca[2], Bollati Carlotta[1], Boschin Giovanna[1], Ranaldi Giulia[3], Ferruzza Simonetta[3], Sambuy Yula[3], Galaverna Gianni[2], Arnoldi Anna[1]

1. Department of Pharmaceutical Sciences, University of Milan, Milan, Italy

2. Department of Food and Drug, University of Parma, Parma, Italy.

3. CREA, Food and Nutrition Research Centre, Rome, Italy

*Corresponding author: Phone: +39-0250319912; FAX: +39-0250319372; Email: carmen.lammi@unimi.it.

Abstract

LTFPGSAED (P7) is a multifunctional hypocholesterolemic and hypoglycemic lupin peptide. While assessing its ACE-inhibitory activity, it was more effective in intestinal Caco-2 cells (IC_{50} 13.7 µM) than in renal HK-2 cells (IC_{50} 79.6 µM). This discrepancy was explained by the metabolic transformation mediated by intestinal peptidases, which produced two main detected peptides, TFPGSAED and LTFPG. Indeed LTFPG, dynamically generated by intestinal DPP-IV, as well as its parent peptide P7 were linearly absorbed by mature Caco-2 cells. An *in silico* study demonstrated that the metabolite was a better ligand of the ACE enzyme than P7. These results are in agreement with an *in vivo* study, previously performed by Aluko et al., which has shown that LTFPG is an effective hypotensive peptide. Our work highlights the dynamic nature of bioactive food peptides that may be modulated by the metabolic activity of intestinal cells.

Keywords: ACE, bioactive peptides, DPP-IV, hypotensive, intestinal transport, peptide.

INTRODUCTION

Recent literature indicates that some peptides obtained through the hydrolysis of different food proteins may provide favorable effects in the area of cardiovascular disease prevention, since they are characterized by hypocholesterolemic, hypoglycemic, or hypotensive activities.[1] Among these peptides those providing more than one activity are classified as multifunctional and are currently considered particularly interesting for practical applications.[2]

In order to express their activity *in vivo*, peptides masked within a protein sequence need not only be released by specific and selective proteases, but also may be absorbed at intestinal level, and enter blood circulation to reach the target organs.[2] Differentiated Caco-2 cells still represent the best available model system for intestinal transport studies.[3,4,5] In fact, when these cells are differentiated on a permeable filter, they form a two-compartments system, where the apical (AP) compartment reproduces the intestinal lumen and the basolateral (BL) one the interstitial space.[6] Recently, an evaluation of the trans-epithelial transport of a peptic lupin hydrolysate[7] has shown that eight peptides are transported across the intestinal cells.[6] One of these peptides was the nonapeptide LTFPGSAED, also named P7.[8] Subsequent experiments have shown that P7 is a multifunctional peptide, since it is able to modulate cholesterol metabolism through inhibition of 3-hydroxy-3-methylglutaryl coenzyme A reductase (HMGCoAR)[8] as well as to regulate glucose metabolism through dipeptidyl peptidase IV (DPP-IV) inhibition.[8-10] Specifically, P7 reduces *in vitro* the activity of HMGCoAR in a dose-response manner and an IC_{50} of 68.4 μM. In human hepatic HepG2 cells, this inhibition leads to an up-regulation of the low density lipoprotein (LDL) receptor (LDLR) protein levels, through the activation of the sterol regulatory element-binding protein 2 (SREBP-2) pathway, and to an increase of LDL absorption from the extracellular environment, with a final hypocholesterolemic effect.[8] In the area of diabetes prevention, P7 impairs the DPP-IV activity in different model systems: specifically, *in vitro* on the DPP-IV enzyme

where the IC_{50} was equal to 228 µM,[10] in human intestinal Caco-2 cells with an IC_{50} of 223 µM, and on the circulating DPP-IV form in human serum with an activity reduction of 18.1% and 24.7% at the concentration of 100 and 300 µM, respectively.[9]

In order to further explore the potential multifunctional behavior of P7, the first objective of this work was an evaluation of its capacity to inhibit the activity of the angiotensin converting enzyme (ACE-1, peptidyl dipeptidase A, EC 3.4.15.1), a key enzyme for blood pressure regulation. Therefore, a preliminary screening of the structures of P7 using BIOPEP (www.uwm.edu.pl/biochemia) had suggested that it might be compatible with a potential behavior as ACE inhibitors. Thus, lupin peptide activity as ACE inhibitor was tested by using two human cellular models, the former based on renal HK-2 cells, an immortalized proximal tubule epithelial cell line from normal adult human kidney, and the latter based on undifferentiated human intestinal Caco-2 cells, a reliable model of the enterocytes. Both cell systems are among those that mostly express ACE in the body. Even though the somatic ACE enzyme expressed by intestinal and renal cells do not seem to directly correlate with blood pressure regulation, it has the same sequence of the ACE expressed in the lung.

The fact that P7 was a more efficient ACE inhibitor in the Caco-2 cellular system than in the renal cellular system has suggested the hypothesis of a metabolic transformation of P7 in one or more active metabolites induced by Caco-2 cells, which are metabolically more active than renal cells. The second objective of the work was thus a study on the behavior of P7 in a differentiated Caco-2 cells model system aimed at investigating the intestinal cellular uptake as well as the possible concurrent degradation by active peptidases, expressed on the AP membranes, which may be accountable for the production of metabolites. After identification of an abundant metabolite, the third objective was to investigate its potential biological activities. In addition, a molecular modeling study was carried out in order to get a deeper comprehension of the interaction of P7 and

its metabolite with the ACE structure. This *in silico* study was based on a structure-based modeling of both ACE domains (namely, the N-domain and C-domain) consisting of pharmacophoric analysis, docking simulations, rescoring procedures, and molecular dynamics.

MATERIALS AND METHODS

Chemicals and reagents. All reagents and solvents were purchased from commercial sources and used without further purification. For further details, see Supplementary Materials.

Cellular ACE-inhibitory assays. HK-2 from ATCC were cultured using Dulbecco Minimum Essential Medium-F12 (DMEM-F12) containing 25 mM glucose, 4 mM stable L-glutamine, 100 U L-1 penicillin, 100 µg L-1 streptomycin, supplemented with 10% heat-inactivated fetal bovine serum (FBS Hyclone Laboratories, Logan, UT, USA). Caco-2 cells, obtained from Institut National de la Santé et de la Recherche Médicale (INSERM, Paris), were routinely sub-cultured at 50% density and maintained at 37 °C in a 90% / 10% air / CO_2 atmosphere in DMEM containing 25 mM glucose, 3.7 g/L $NaHCO_3$, 4 mM stable L-glutamine, 1% non-essential amino acids, 100 U/L penicillin, 100 µg/L streptomycin (complete medium), supplemented with 10% heat inactivated FBS.[11]

For the experiments, HK-2 and Caco-2 cells were seeded on 96-well plates at a density of 5×10^4 cells/well for 24 h. The following day, cells were treated with 100 µL P7 (0.1-250 µM) or vehicle in growth medium for 24 h at 37 °C. On the next day, cells were scraped in 30 µL of ice-cold ACE1 lysis buffer and transferred into an ice-cold microcentrifuge tube. After centrifugation at 13,300g for 15 min at 4 °C, the supernatant was recovered and transferred into a new ice-cold tube. Total proteins were quantified by Bradford method, and 2 µL of the supernatant (the equivalent of 2 µg of total proteins) were added to 18 µL of ACE1 lysis buffer in each well in a black 96-well plate with

clear bottom. For the background control, 20 µL of ACE1 lysis buffer were added to 20 µL of ACE1 assay buffer. Then, 20 µL of diluted ACE1 substrate [o-aminobenzoyl peptide (Abz based peptide) substrate, 4% of ACE1 substrate in assay buffer] was added in each well except the background one, and the fluorescence (Ex/Em 330/430 nm) was measured in a kinetic mode for 10 min at 37 °C.

Caco-2 cell culture and differentiation. For differentiation, Caco-2 cells were seeded on polycarbonate filters, 12 mm diameter, 0.4 µm pore diameter (Transwell, Corning Inc., Lowell, MA, US) at a 3.5×10^5 cells/cm^2 density in complete medium supplemented with 10% FBS in both AP and BL compartments for 2 d to allow the formation of a confluent cell monolayer. Starting from day three after seeding, cells were transferred to FBS-free medium in both compartments, supplemented with ITS [final concentration 10 mg/L insulin (I), 5.5 mg/L transferrin (T), 6.7 µg/l sodium selenite (S); GIBCO-Invitrogen, San Giuliano Milanese, Italy] only in the BL compartment, and allowed to differentiate for 18-21 days with regular medium changes three times weekly.[12]

Cell monolayers integrity evaluation. The transepithelial electrical resistance (TEER) of differentiated Caco-2 cells was measured at 37 °C using the voltmeter apparatus Millicell (Millipore Co., USA,), immediately before and at the end of the transport experiments. In addition, at the end of transport experiments, cells were incubated from the AP side with 1 mM phenol-red in PBS containing Ca^{++} (0.9 mM) and Mg^{++} (0.5 mM) for 1 h at 37 °C, to monitor the paracellular permeability of the cell monolayer. The BL solutions were then collected and NaOH (70 µL, 0.1 N) was added before reading the absorbance at 560 nm by a microplate reader Synergy H1 from Biotek (Winooski, VT, USA). Phenol-red passage was quantified using a standard phenol-red curve. Only

filters showing TEER values and phenol red passages similar to untreated control cells were considered for peptide transport analysis.

Trans-epithelial transport of P7 and LTFPG. Prior to experiments, the cell monolayer integrity and differentiation were checked by TEER measurement as described in detail above. Cells were then washed twice, and peptide transportation by intestinal cells assayed. Transport experiments were performed in transport buffer solution (137 mM NaCl, 5.36 mM KCl, 1.26 mM $CaCl_2$, and 1.1 mM $MgCl_2$, 5.5 mM glucose) following conditions previously described.[13] In order to reproduce the pH conditions existing *in vivo* in the small intestinal mucosa, AP solutions were maintained at pH 6.0 (buffered with 10 mM morpholinoethane sulfonic acid), and BL solutions were maintained at pH 7.4 (buffered with 10 mM N-2-hydroxyethylpiperazine-N-4-butanesulfonic acid). Prior to transport experiments, cells were washed twice with 500 µL PBS containing Ca^{++} and Mg^{++}. Peptide transportation by mature Caco-2 cells was assayed by loading the AP compartment with P7 and/or LTFPG (500 µM) in the AP transport solution (500 µL) and the BL compartment with the BL transport solution (700 µL). The plates were incubated at 37 °C and the BL solutions were collected at different time points (i.e. 15, 30, 60, 90, and 120 min) and replaced with fresh solutions prewarmed at 37 °C. All BL solutions together with the AP solutions collected at the end of the transport experiment were stored at -80 °C prior to analysis. Three independent transport experiments were performed, each in duplicate.

Targeted HPLC-Chip-MS/MS analysis: method set−up and validation. Quantitative analysis of P7 in the AP and BL samples were carried out by the Ion Trap MS in multiple reaction monitoring (MRM) mode, monitoring two of the most intense diagnostic transitions, after optimization of the acquisition parameters, such as retention time, MS profile, and MS/MS fragmentation spectrum.[14,

[15] All further details regarding LC-MS/MS operating conditions and method validations are described in Supplementary Materials.

Untargeted HPLC-Chip-MS/MS analysis for the detection of metabolites. The metabolic degradation products deriving from the hydrolytic activity of brush border membrane peptidases were investigated by an untargeted approach (for further details see Supplementary Materials). Briefly, the extraction of MS/MS spectra for the metabolite analysis was conducted accepting a minimum sequence length of 3 amino acids and merging scans with same precursor within a mass window of ±0.4 m/z in a time frame of ±5 s. Methionine oxidation, acetylation (K), pyroglutamic acid (N-termQ), deamidated (N) were set as variable modifications, no enzyme was chosen as digestive enzymes; 2 missed cleavage were allowed. MS/MS search was conducted against the subset of *Lupinus* protein sequences (8669 entries) downloaded from UNIProtKB (http://www.uniprot.org/). The mass tolerance of parent and fragments of MS/MS data search was set at 1.0 Da for precursor ions and 0.8 for fragment ions, respectively. The autovalidation strategy both in peptide mode and in protein polishing mode was performed using FDR cut-off ≤ 1.2%.

Stability of P7 in the presence of DPP-IV. The experiments were carried out in microcentrifuge tubes. Each reaction (100 µL) was prepared by adding the reagents in the following order: 1 × DPP-IV assay buffer [20 mM Tris-HCl, pH 8.0, containing 100 mM NaCl, and 1 mM EDTA] (80 µL), P7 solution (10 µL, 500 µM) and finally DPP-IV (10 µL). Subsequently, the samples were mixed and kept at 37 °C in a thermoblock for 5, 30, and 120 min. At the end of the reactions, DPP-IV was inactivated by adding 200 µL of precooled ACN to each tube, then the samples were centrifuged for 10 min at 13,300g at 4 °C and the supernatant collected. P7 and LTFPG were loaded onto the enrichment column (Zorbax 300SB-C18, 5 µm pore size) at a flow rate 4 µL/min using isocratic

100% C solvent phase (99% water, 1% ACN and 0.1% formic acid). After the clean-up, P7 and LTFPG were separated on a 150 mm × 75 µm analytical column (Zorbax300SB-C18, 5 µm pore size) at the constant flow rate of 300 nL/min. The LC solvent A was 95% water, 5% ACN, 0.1% formic acid; solvent B was 5% water, 95% ACN, 0.1% formic acid. The nano-pump gradient program was as follows: 5% solvent B (0 min), 70% solvent B (0–8 min), and back to 5% in 2 min. Post-time was 10 mins. The drying gas temperature was 300 °C, flow rate 3 L/min (nitrogen). Data acquisition occurred in positive ionization mode. Capillary voltage was −1950 V, with endplate offset −500V. Mass spectra were acquired under MRM conditions by monitoring the m/z 469.8 and 534,2 for P7 and LTFPG, respectively.

In vitro DPP-IV inhibitory activity assay. The experiments were carried out in a half volume 96 well solid plate (white) with LTFPG at the final concentration of 10, 100, and 500 µM and using conditions previously optimized.[10] For further details, see Supplementary Materials

In vitro assessment of the HMGCoAR inhibitory activity. The assay buffer, NADPH, substrate solution, and HMGCoAR were provided in the HMGCoAR Assay Kit (Sigma). The experiments were carried out testing LTFPG at 100 and 250 µM at 37 °C in agreement with the conditions previously reported[8]. For further details, see Supplementary Materials.

In silico study. The molecular modeling study aimed at describing the interaction of peptides with both the N- and C-domain of human ACE. The study relied on pharmacophore modeling, docking studies and molecular dynamic simulations, as detailed below.

Model Preparation. The models for the C- and N-domain of human ACE were derived from the three-dimension structures recorded into the Protein Data Bank (http://www.rcsb.org) with PDB

codes 4APH and 4BZS, respectively.[16, 17] Protein structures were processed using the software Sybyl, version 8.1 (www.certara.com), as previously reported.[18] Briefly, all atoms of both structures were checked for atom- and bond-type assignments and amino- and carboxyl-terminal groups were set as protonated and deprotonated, respectively. Hydrogen atoms were computationally added to the protein and energetically minimized using the Powell algorithm (the coverage gradient was set ≤0.5 kcal/(mol Å) with a maximum of 1500 cycles). All sets of small molecules, but not the Zn ions, co-crystallized within the catalytic sites were removed to prepare the model for docking simulations. Peptides were designed using the "Build Protein" tool of the "Biopolymer" module of Sybyl, version 8.1 (www.certara.com). Then, they were energetically minimized using the Powell algorithm with a coverage gradient ≤ 0.05 kcal/(mol Å) and a maximum of 500 cycles.

Pharmacophoric modeling. The pharmacophoric modeling aimed at describing the physicochemical properties of catalytic sites in terms of distribution of hydrophobic and hydrophilic features. The binding site of both domains of ACE was defined using the Flapsite tool of the FLAP software while the GRID algorithm was used to investigate the corresponding pharmacophoric space.[19, 20] In particular, the DRY probe was used to describe potential hydrophobic interactions, while the sp2 carbonyl oxygen (O) and the neutral flat amino (N1) probes were used to describe the hydrogen bond acceptor and donor capacity of the target, respectively.

Docking study and rescoring procedure. The docking study aimed at investigating the architectures of peptide binding within the catalytic sites of ACE domains. The GOLD software (version 5.7)[21] was used to perform all of the docking simulations, while a rescoring procedure using the HINT scoring function[22] was performed for the better evaluation of the peptide-ACE interaction. In particular, HINT score relates to the free energy of binding (the higher the score means the stronger the interaction, while negative scores indicate the lack of appreciable interaction).[23] Notably, the coupling of docking simulations using GOLD and rescoring procedures using HINT already

succeed in identifying enzymes inhibitors as previously showed.[23-25] Software setting and docking protocol were used as reported previously.[25] Briefly, the explorable space available for docking peptides was set at 10 Å around the Zn ion. In addition, the interaction of C-terminal carboxylic group of peptides was restrained in agreement with the arrangement of carboxylic group of captopril, as reported by crystallographic study,[26] to speed up the spatial search.

GOLD uses a Lamarckian genetic algorithm, and scores may slightly change from run to run. Therefore, to exclude a non-causative score assignment, simulations were run in quintuplicate, and the mean values are reported, in agreement with previous studies.[25]

Molecular dynamic simulations. Molecular dynamic (MD) simulations were performed to study the dynamic of interactions between peptides and the ACE domains over time. The best scored binding poses calculated by docking simulations were used as input for MD. MD simulations were performed using GROMACS (version 5.1.4) with CHARMM27 all-atom force field parameters support,[27] in agreement with a previous study.[28] Briefly, protein-peptide complexes solvated with SPCE waters in a cubic periodic boundary condition, and counter ions (Na^+ and Cl^-) were added to neutralize the system. Prior to MD simulation the systems were energetically minimized to avoid steric clashes and to correct improper geometries using the steepest descent algorithm with a maximum of 5000 steps. Afterwards, all the systems underwent isothermal (300 K, coupling time 2psec) and isobaric (1 bar, coupling time 2 psec) 100 psec simulations before running 50 nsec simulations (300 K with a coupling time of 0.1 psec and 1 bar with a coupling time of 2.0 psec).

Statistical analysis. All LC-MS analysis were run in triplicate on each biological replicate. Statistical analysis, including determination of linear regression, average, standard deviation (s.d.) and coefficient of variance (CV), was performed using Graphpad Prism 7 (GraphPad Software, La Jolla, CA, USA). Values were expressed as means ± s.d.. For the experiments aimed at evaluating

the bioactivity of P7 and LTFPG, statistical analyses were carried out by One-way ANOVA (Graphpad Prism 7), followed by Brown-Forsythe's test. Values were expressed as means ± s.d.; P-values < 0.05 were considered to be significant.

RESULTS

P7 inhibits the ACE activity expressed by human renal cells and intestinal Caco-2 cells in different ways. In order to get a deeper characterization of the multifunctional behavior of P7, its ACE inhibitory activity was investigated using a cell-based assay recently optimized in our laboratory, which is based on human renal HK-2 and intestinal Caco-2 cells.[29] After treatment of both cell systems with P7, the ACE activity was measured directly in the cell lysates using a fluorescent ACE substrate: in this assay, the fluorescent signal is proportional to the enzyme activity. As shown in Figure 1, P7 inhibited the enzyme activity in both renal HK-2 and Caco-2 cell systems with a dose-response trend and IC_{50} values equal to 79.6±0.20 μM and 13.7±0.28 μM, respectively, i.e. P7 is 6-fold more active at intestinal than at renal level.

The differences between the results in the two cellular systems may be possibly explained considering the propensity of P7 to undergo a metabolic degradation by active peptidases. In fact, the different metabolic pattern of each cell line may be responsible for the generation of one or more break-down fragments each endowed with specific activities that may be different from those of the parent peptide. It was thus hypothesized that the metabolic activities expressed by the Caco-2 cells and, in particular, the hydrolytic activity of brush border peptidases might actively influence the behavior of P7 through the production of smaller metabolic fragments, which might be more active than the parent peptide. Therefore, the subsequent in-depth experimentation was aimed at getting a solid explanation of this phenomenon by evaluating the behavior of P7 in presence of mature intestinal Caco-2 cells.

Transport and metabolism of P7 alone or in mixture with other peptides across Caco-2 cells.

The following experiments were dedicated evaluating the transport and metabolism of P7 in differentiated Caco-2 cells monolayers. From a dynamic point of view, the transport process of bioactive peptides may be different when they are present in a complex hydrolysate or when they are alone. For this reason, it was decided to investigate the kinetics of P7 transport in two different conditions, i.e. when P7 was alone or when it was in mixture. The mixture was prepared by mixing P7 with two other lupin peptides, namely YDFYPSSTKDQQS (P3) and LILPKHSDAD (P5), which had been already demonstrated to be transported in the same system. Each peptide was tested at the concentration of 500 μM in the AP compartment.

As shown in Figure 2, in both systems, P7 was linearly absorbed across the Caco-2 cells monolayer as a function of time. In the case of P7 alone, the rate of transport was 4.2 ±0.6 ng/(mL × min) (R^2 0.999), with a lag period for transport of 0.5 min, whereas in mixture the rate was 1.98 ± 0.21 ng/(mL × min) (R^2 0.955), with a lag period of 27.7 min (Figure 2). The much slower rate observed when P7 was in mixture suggests that peptide-peptide or peptide-peptidases interactions actively modulate the dynamic of its transport. In fact, the presence of other peptides may preferentially favor a certain transport selectivity. Moreover, after 60 min of incubation, the amount of P7 in the BL compartment was about 4-fold higher (0.26 ±0.02 μg, equal to 0.278 nmoles) when it was tested alone than when it was tested in the mixture (0.06 ±0.003 μg, equal to 0.064 nmoles). Moreover, in the latter conditions, 2 h were required in order to reach about the same absorbed amount (0.22±0.5 μg, 0.235 nmoles). In all cases, the incubation with the peptides did not affect the monolayer integrity as monitored by TEER values and phenol red passage (data not shown), thus indicating that the passage was transcellular rather than paracellular.

Analysis of the metabolites produced by Caco-2 cells. In their AP sides, mature enterocytes develop functional structures, the microvilli, on whose surface many active carriers and metabolic enzymes are expressed. In the same way, differentiated Caco-2 cells express in their AP membrane a wide range of peptidases, including also DPP-IV and ACE. From a physiological point of view, the dynamic equilibrium between bioactive peptides transport and degradation is crucially important. Therefore, under the hypothesis that the low transport rate observed for P7 might be attributed to competing *in situ* degradation by the hydrolytic activity of brush border peptidases, the AP solutions, collected after 120 min of the transport experiment, were analyzed looking for metabolic degradation products. Two peptides, namely TFPGSAED (with m/z 823.20) and LTFPG (with m/z 534.29), were identified deriving from the loss of the first amino acid (L) from the N-terminal side and the loss of the last four amino acids residue (SAED) from the C-terminal side, respectively (Table 1). These results suggest that P7 is a substrate of two different peptidases: leucine aminopeptidase (LAP) catalyzes the hydrolysis of the leucine residues at the N-terminus of P7 generating the TFPGSAED, while among all the intestinal endo-peptidases, DPP-IV might be responsible for the formation of the LTFPG fragment. The fact that both metabolites are detected only in the AP samples of the experiments when P7 is tested in mixture underlines different kinetics in the generation of breakdown fragments. Possibly, the presence of other peptides in the AP compartment may protect the two major metabolites from further degradation by the intestinal peptidase that express their activities on different substrates. The fact that, when it is tested in mixture, P7 can be detected in the BL medium only after 27 min, suggests that over that period of time the degradation into the two metabolites prevails over transport. Possibly, protected by the presence of the other peptides against degradation, the metabolites might impair the P7 transport thus delaying its passage and detection in the BL medium. However, the confirmation of this hypothesis would require further studies. Conversely, when P7 is individually tested, it is rapidly

absorbed, without lag period, and its major metabolites are not detectable in the AP medium at the end of the experiment (60 min), possibly due to their total degradation by intestinal peptidases, generating smaller break-down fragments that are intrinsically difficulty to assign, such as tri- and di-peptides. Alternatively, the cited metabolites might have been produced but remain below the detection limit.

LTFPG is a metabolic product of the intestinal DPP-IV activity. The following investigations were focused on LTFPG, since TFPGSAED is very similar to the parent peptide P7. In order to verify whether DPP-IV was responsible for the production of LTFPG from P7, an *in vitro* biochemical test was performed using the purified recombinant enzyme. P7 (500 μM) was incubated with DPP-IV for 5, 30, and 120 min and the formation of LTFPG was monitored by LC-MS. LTFPG was clearly detectable after 2 h of incubation as indicated by Figure 3A that reports the total ion current (TIC) and extracted ions current (EIC) chromatograms of P7 and LTFPG. The tandem MS spectra of LTFPG is shown in Figure 3B. As indicated by Figure 3C, the peak area of LTFPG increases as a function of incubation time.

In addition, a transport experiment was performed using mature Caco-2 cells (Figure 3D): the rate of transport of LTFPG alone (incubated in the AP compartment at the concentration of 500 μM) was equal to 3.7 ±0.8 ng/(mL × min) (R^2 0.997) without lag period. Interestingly, after 60 min of transport, the concentration of LTFPG in the BL compartment (0.22 ±0.003 μg, equal to 0.412 nmoles) was much higher than that of the parent peptide P7 tested alone (0.26 ±0.02 μg, equal to 0.278 nmoles). This result suggests that LTFPG is either efficiently transported or poorly metabolized by intestinal Caco-2 cells. Additional experiments showed that LTFPG is transported also in the presence of wortmannin, a well-known inhibitor of the transcellular passage (see Figure 1S), suggesting that the mechanism of transport may involve the paracellular route. It is important

to underline, however, that dedicated experiments would be required for a complete characterization of the LTFPG transport mechanism.

In silico studies of the ACE-inhibitory properties of P7 and its metabolite. Recent literature indicates that indeed LTFPG is a hypotensive peptide. In particular, Aluko and co-workers have identified this peptide after the hydrolysis of pea seed provicilin with thermolysin[30] and have demonstrated that it has moderate but significant *in vitro* inhibitory activities on ACE and renin. Moreover, when orally administered to SHR at a dose of 30 mg/kg body weight, LTFPG produces a fast and efficient decrease in systolic blood pressure with a maximum of -37 mmHg after 2 h. These results demonstrate a hypotensive activity

Based on these considerations, an in silico study was carried out in order to compare the mechanisms through which P7 and LTFPG interact with the ACE enzyme, using a molecular modeling approach, in agreement with a previous study.[25] Briefly, an integrated use of docking simulations, rescoring procedures, pharmacophoric analysis, and molecular dynamic simulations were used to estimate the capacity of peptides to favorably and stably interact with the two catalytic sites of the enzyme.

In more detail, docking simulations provided the binding poses of the peptide, which were rescored using the HINT scoring function to find the most likely and favored one. The coupled use of docking simulations and HINT as re-scoring function was chosen, as it previously succeeded to estimate the favors of peptide-enzyme complex formation.[25, 31] In particular, HINT score may correlate to the favors of binding, as previously reported (the higher the score, the more favored the expected interaction).[23]

P7 showed negative HINT scores within both sites (-932 and -1810 units within the N- and C-domains, respectively), suggesting a low fitting within the two catalytic sites of ACE. This evidence

was in line with its moderate *in vitro* ACE inhibitory activity (10.9±0.95% at 1.0 mg/mL), as mentioned above (see Table 1S in Supplementary Materials). Therefore, P7 was not investigated further in the computational assessment.

Conversely, LTFPG showed relatively high and positive scores in both catalytic sites (975 and 426 HINT score units within t N- and C-terminal domain, respectively) suggesting a theoretical fitting higher than that of P7. This result is in accordance to the higher activity of LTFPG with respect to the parent peptide P7, and it clearly points to the higher capability of the former to better satisfy the physico-chemical requirements of ACE catalytic sites. The analysis of the poses revealed that LTFPG had a very similar architecture of binding in both sites with the exception of a slightly different arrangement of its N-terminal residues among the two. This result may explain the diverse scores observed in the two sites. The analysis of molecular dynamics results showed a slightly different behavior of LTFPG between the two catalytic sites (Figure 4B). In particular, the root-mean-square deviation (RMSD) analysis was used to monitor the geometrical stability within the two catalytic sites over the time, in agreement with previous study. The results collected showed stable interaction of LTFPG within the catalytic site of the N-terminal from the half of simulation on as it showed a steady geometry from 25 ns until the end of the simulation. Conversely, within the C-domain, LTFPG showed a discrete increase of RMSD in the last part of the simulation, though showing a steady geometry until the end of simulation. In addition, the analysis of LTFPG trajectories showed its capability to persist within the two catalytic sites over the time. Specifically, concerning the interaction with the catalytic site of the ACE N-domain, the reorganization of the N-terminus of LTFPG along the simulation explained the high RMSD values observed in the first part of the simulation. Overall, the results collected pointed to the capability of LTFPG to interact and stably persist within both the catalytic sites of ACE.

Evaluation of the inhibitory activity of LTFPG on DPP-IV and HMGCoAR. It was decided to verify whether LTFPG retained the multifunctional activities of the parent compound P7. The results of these experiments showed that LTFPG loses the ability to reduce the *in vitro* activity of DPP-IV (Figure 5A), whereas it maintains a modest ability to reduce the *in vitro* HMGCoAR activity. In fact, it inhibits the enzyme by 4.7±0.3% and 10.3±0.8% at 100 and 250 μM Figure 5B).

DISCUSSION

Although there is an increasing number of papers that underline the interesting biological properties of food peptides, the issue of their metabolism and transport still remain a relevant issue of discussion. In particular, these phenomena have been invocated to explain the discrepancy observed between *in vitro* assays and *in vivo* results. For example, there are many reports in the literature on the ACE-inhibitory activity of different food-derived peptides.[32] In all these studies, the biochemical characterization is carried out using tests on the purified recombinant ACE enzymes from lung or kidney of different animal species, such as pig and rabbit. These biochemical tools, involving a purified ACE enzyme and a standard substrate, provide only an incomplete characterization of the activity and represent a rudimental way of screening, which does not always correlate with the hypotensive effect observed in experimental studies that are usually performed using spontaneously hypertensive rats (SHR) as the model system. For example, IQW and LKP are two peptides deriving from a thermolysin–pepsin ovotransferrin hydrolysate. IQW seems the better ACE-inhibitor in the biochemical test, having an IC_{50} value equal to 1.56 μM versus 2.93 μM of LKP, but when they are tested *in vivo* in the SHR model, IQW is the less effective, since it induces a -21.0 mmHg decrease of the BP, whereas LKP induces a -30.0 mmHg decrease.[33, 34] Recently, three peptides, WYT, SVYT, and IPAGV, identified in a hempseed hydrolysate, have been shown to exert an *in vitro* ACE-inhibitory activity of 89.0%, 79.0%, and 60.0% at 0.5 mg/mL, respectively.

However, IPAGV, the least active *in vitro*, was the most active in reducing the BP of SHR (−40.0 mmHg).[35] Moreover, FKGRYYP, LKP, and IKW, three peptides identified from meat derived hydrolysates obtained using thermolysin, are totally ineffective *in vivo* on SHR, although they reduce *in vitro* the ACE activity with IC_{50} values equal to 0.55, 0.32, and 0.21 μM, respectively.[36]

In addition, more and more works underline the possibility that in some cases metabolism may generate a fragment whose activity is enhanced and/or shifted to different targets. This is the case of peptide P7 that in itself is a poor inhibitor of the ACE activity (as also shown here by *in silico* outcomes), whereas the metabolic transformation induced by DPP-IV produced the active peptide LTFPG, whose hypotensive activity has been demonstrated either *in vitro* or *in vivo* in the SHR model. [30]

The DPP-IV ability to generate the active LTFPG fragment, after P7 degradation, highlights an additional aspect of the previously described DPP-IV inhibitory nature of P7.[9, 10] In general, three modes are used to describe the nature of enzyme inhibition: true, substrate, and prodrug type.[37] True inhibitors are not degraded during incubation with the enzyme, whereas substrate and prodrug inhibitors are metabolized by the enzyme. DPP-IV inhibitors are classified on the basis of their stability to the hydrolytic action of DPP-IV *per se*.[38] In this context, our results clearly confirm that P7 is a substrate of DPP-IV that acts as a competitive inhibitor, since it is subjected to DPP-IV hydrolysis. P7, however, is not a DPP-IV prodrug inhibitor, since LTFPG loses the ability to reduce the *in vitro* DPP-IV enzyme activity (Figure 5A). Recently, a molecular docking study has investigated the P7 interaction within the catalytic site of the DPP-IV enzyme.[10] Results suggest that the P7 C-terminal interacts with Arg358 and Arg356 and is engaged in an extended ionic network, also involving the side-chain of the C-terminal residue (Asp9 in P7) and Arg429. Moreover, the contacts stabilized by the N-terminal elicits the already described ion-pairs with Glu205 and Glu206 in the active peptide P7. Finally, P7 includes an aromatic residue (Phe3)

engaged in a rich set of π–π stacking involving Tyr547, Trp629, and His740.[10] Thus, it is clear that even though P7 metabolite may potentially interact through the N-terminal residues with the catalytic side of the enzyme, this interaction is not further stabilized by the C-terminal of the peptide, explaining why LTFPG does not act as DPP-IV prodrug inhibitor.

Differently, LTFPG maintains a modest ability to reduce *in vitro* the HMGCoAR activity (by 4.7±0.3% and 10.3±0.8% at 100 and 250 μM, respectively), however it is much less potent than the parent peptide P7 (IC_{50} of 68.4 μM).[8] In order to function as a competitive inhibitor of HMGCoAR, a peptide should mimic the hydroxymethylglutaryl moiety. To achieve this goal, the conformation and the side chain groups play a more important role than the total hydrophobicity. Moreover, the correlation of the inhibitory activity with the peptide length has not yet been established, while it has been confirmed that a Leu, Ile and/or Tyr residue at the N-terminal and a Glu residue at the C-terminal play important roles for the peptide inhibitory property.[39, 40] In fact, the *in silico* prediction of P7 binding mode within the catalytic site of the enzyme suggests that the P7-HMGCoAR complex may be stabilized by a set of interactions, which can be subdivided into three groups: (1) The positively charged N-terminal elicits ion-pairs with Glu559 and Asp767, reinforced by H-bonds with surrounding Thr557 and Thr558. (2) Negatively charged residues located at C-terminal tail (including the C-terminal itself) are engaged in ionic contacts with Arg568, Arg571, and Lys722. (3) Hydrophobic residues located at N-terminal are involved in hydrophobic interactions with apolar residues (e.g., Leu76, Ile536, Leu562, Met655, and Met657).[6] Thus, it appears that due to the hydrolytic activity of DPP-IV, LTFPG maintains the set of interactions which involve the N-terminal side of the peptide but it drastically loses the important set of interactions between the C-terminal side of the peptide and the Arg568, Arg571, and Lys722, which stabilize the complex peptide-catalytic site of the enzyme, with a consequent reduction of LTFPG inhibitory potency.

In conclusion, the couple P7 and LTFPG represent an exemplary case of the multiple facets of the behavior of some multifunctional peptides: the degradation of P7, which is hypocholesterolemic and hypoglycemic, produces a metabolite that loses these activities but becomes hypotensive. This study underlines how in the field of multifunctional peptides, the overall activities may be attributed to the concomitant presence of metabolites with the same or also new bioactivity. This new vision highlights the dynamic nature of bioactive food peptides that may be modulated by the metabolic activity of intestinal cells. This aspect is still mostly underestimated, since the identification and characterization of multifunctional peptides from food proteins is still addressed using traditional and static approaches.

Abbreviations and Nomenclature

ACE, Angiotensin converting enzyme; **ACN**, Acetonitrile; **AP**, Apical; **BL**. Basolateral; **CV**, coefficient of variance; **DMEM**, Dulbecco's modified Eagle's medium; **DPP-IV**, Dipeptidyl peptidase IV; **EIC**, Extracted ions current; **FBS**, Fetal bovine serum; **HMGCoAR**, 3-hydroxy-3-methylglutaryl coenzyme A reductase; **ITS**, insulin-trasferrin-selenium; **LAP**, leucine aminopeptidase; **LC-MS/MS**, Liquid chromatography-mass spectrometry; **LDL**, Low-Density Lipoprotein; **LDLR**, Low-Density Lipoprotein Receptor; **MD**, Molecular dynamic; **MRM**, multiple reaction monitoring; **MS/MS**, Tandem mass spectrometry; **NADPH**, Nicotinamide adenine dinucleotide phosphate; **PBS**, Phosphate buffered saline; **PDB**, Protein Data Bank; **RMSD**, Root-mean-square deviation; **s.d.**, Standard deviation; **SHR,** Spontaneously hypertensive rats; **SREBP-2**, Sterol regulatory element-binding protein 2; **TEER**, The transepithelial electrical resistance; **TIC**, Total ion current.

Author contributions

Experiment ideation C.L; Biological experiments, C.L. S.F. G.R., C.B., and G.B.; Analytical Experiments: G.A.; Computational Experiments: L.D. Data analysis, C.L. L.D. and G.A.; Discussion of the results, C.L. and L.D.; Manuscript writing, C.L. L.D. G.G.Y.S. and A.A.

Acknowledgments

The authors gratefully acknowledge Carlo Sirtori Foundation (Milan, Italy) for having provided part of the equipment used in this experimentation. Moreover, this research benefits from the HPC (high performance computing) facility of the University of Parma, Italy. The authors would like also to acknowledge Prof. Pietro Cozzini and Glen E. Kellogg for the courtesy of HINT scoring function and Gabriele Cruciani for the courtesy of FLAP software (www.moldiscovery.com).

Supporting Information. Information of chemicals and reagents used in this study. Technical details of *in vitro* experiments and HPLC-Chip-MS/MS analysis

References

1. Chakrabarti, S.; Guha, S.; Majumder, K., Food-derived bioactive peptides in human health: challenges and opportunities. *Nutrients* **2018,** *10* (11).

2. Lammi, C.; Aiello, G.; Boschin, G.; Arnoldi, A., Multifunctional peptides for the prevention of cardiovascular disease: A new concept in the area of bioactive food-derived peptides. *J Funct Foods* **2019,** *55*, 135-145.

3. Cabanos, C.; Kato, N.; Amari, Y.; Fujiwara, K.; Ohno, T.; Shimizu, K.; Goto, T.; Shimada, M.; Kuroda, M.; Masuda, T.; Takaiwa, F.; Utsumi, S.; Nagaoka, S.; Maruyama, N., Development of a novel transgenic rice with hypocholesterolemic activity via high-level accumulation of the alpha' subunit of soybean beta-conglycinin. *Transgenic Res* **2014,** *23* (4), 609-620.

4. Meunier, V.; Bourrié, M.; Berger, Y.; Fabre, G., The human intestinal epithelial cell line Caco-2; pharmacological and pharmacokinetic applications. *Cell Biol Toxicol* **1995,** *11* (3-4), 187-94.

5. Sambuy, Y.; De Angelis, I.; Ranaldi, G.; Scarino, M. L.; Stammati, A.; Zucco, F., The Caco-2 cell line as a model of the intestinal barrier: influence of cell and culture-related factors on Caco-2 cell functional characteristics. *Cell Biol Toxicol* **2005,** *21* (1), 1-26.

6. Lammi, C.; Aiello, G.; Vistoli, G.; Zanoni, C.; Arnoldi, A.; Sambuy, Y.; Ferruzza, S.; Ranaldi, G., A multidisciplinary investigation on the bioavailability and activity of peptides from lupin protein. *J Funct Foods* **2016,** *24*, 297-306.

7. Lammi, C.; Zanoni, C.; Scigliuolo, G. M.; D'Amato, A.; Arnoldi, A., Lupin peptides lower low-density lipoprotein (LDL) cholesterol through an up-regulation of the LDL receptor/sterol regulatory element binding protein 2 (SREBP2) pathway at HepG2 cell line. *J Agric Food Chem* **2014,** *62* (29), 7151-9.

8. Zanoni, C.; Aiello, G.; Arnoldi, A.; Lammi, C., Investigations on the hypocholesterolaemic activity of LILPKHSDAD and LTFPGSAED, two peptides from lupin beta-conglutin: Focus on LDLR and PCSK9 pathways. *J Funct Foods* **2017,** *32*, 1-8.

9. Lammi, C.; Bollati, C.; Ferruzza, S.; Ranaldi, G.; Sambuy, Y.; Arnoldi, A., Soybean- and lupin-derived peptides inhibit DPP-IV activity on in situ human intestinal Caco-2 Cells and ex vivo human serum. *Nutrients* **2018,** *10* (8).

10. Lammi, C.; Zanoni, C.; Arnoldi, A.; Vistoli, G., Peptides derived from soy and lupin protein as Dipeptidyl-Peptidase IV inhibitors: *In vitro* biochemical screening and *in silico* molecular modeling study. *J Agric Food Chem* **2016,** *64* (51), 9601-9606.

11. Natoli, M.; Leoni, B. D.; D'Agnano, I.; D'Onofrio, M.; Brandi, R.; Arisi, I.; Zucco, F.; Felsani, A., Cell growing density affects the structural and functional properties of Caco-2 differentiated monolayer. *J Cell Physiol* **2011,** *226* (6), 1531-43.

12. Ferruzza, S.; Rossi, C.; Sambuy, Y.; Scarino, M. L., Serum-reduced and serum-free media for differentiation of Caco-2 cells. *ALTEX* **2013,** *30* (2), 159-68.

13. Lammi, C.; Zanoni, C.; Ferruzza, S.; Ranaldi, G.; Sambuy, Y.; Arnoldi, A., Hypocholesterolaemic activity of lupin peptides: Investigation on the crosstalk between human enterocytes and hepatocytes using a co-culture system including Caco-2 and HepG2 cells. *Nutrients* **2016,** *8* (7).

14. Lammi, C.; Zanoni, C.; Aiello, G.; Arnoldi, A.; Grazioso, G., Lupin peptides modulate the protein-protein interaction of PCSK9 with the low density lipoprotein receptor in HepG2 cells. *Sci Rep* **2016,** *6*, 29931.

15. Lammi, C.; Zanoni, C.; Arnoldi, A.; Aiello, G., YDFYPSSTKDQQS (P3), a peptide from lupin protein, absorbed by Caco-2 cells, modulates cholesterol metabolism in HepG2 cells via SREBP-1 activation. *J Food Biochem* **2018,** *42* (3), 8.

16. Kramer, G. J.; Mohd, A.; Schwager, S. L.; Masuyer, G.; Acharya, K. R.; Sturrock, E. D.; Bachmann, B. O., Interkingdom pharmacology of Angiotensin-I converting enzyme inhibitor phosphonates produced by actinomycetes. *ACS Med Chem Lett* **2014,** *5* (4), 346-51.

17. Masuyer, G.; Schwager, S. L.; Sturrock, E. D.; Isaac, R. E.; Acharya, K. R., Molecular recognition and regulation of human angiotensin-I converting enzyme (ACE) activity by natural inhibitory peptides. *Sci Rep* **2012,** *2*, 717.

18. Dellafiora, L.; Dall'Asta, C.; Cozzini, P., Ergot alkaloids: From witchcraft till. *Toxicol Rep* **2015,** *2*, 535-545.

19. Baroni, M.; Cruciani, G.; Sciabola, S.; Perruccio, F.; Mason, J. S., A common reference framework for analyzing/comparing proteins and ligands. Fingerprints for Ligands and Proteins (FLAP): theory and application. *J Chem Inf Model* **2007,** *47* (2), 279-94.

20. Carosati, E.; Sciabola, S.; Cruciani, G., Hydrogen bonding interactions of covalently bonded fluorine atoms: from crystallographic data to a new angular function in the GRID force field. *J Med Chem* **2004,** *47* (21), 5114-25.

21. Jones, G.; Willett, P.; Glen, R. C.; Leach, A. R.; Taylor, R., Development and validation of a genetic algorithm for flexible docking. *J Mol Biol* **1997,** *267* (3), 727-48.

22. Eugene Kellogg, G.; Abraham, D. J., Hydrophobicity: is LogP(o/w) more than the sum of its parts? *Eur J Med Chem* **2000,** *35* (7-8), 651-61.

23. Dellafiora, L.; Marchetti, M.; Spyrakis, F.; Orlandi, V.; Campanini, B.; Cruciani, G.; Cozzini, P.; Mozzarelli, A., Expanding the chemical space of human serine racemase inhibitors. *Bioorg Med Chem Lett* **2015,** *25* (19), 4297-303.

24. Marseglia, A.; Dellafiora, L.; Prandi, B.; Lolli, V.; Sforza, S.; Cozzini, P.; Tedeschi, T.; Galaverna, G.; Caligiani, A., Simulated gastrointestinal digestion of cocoa: Detection of resistant peptides and in silico/ in vitro prediction of their ACE inhibitory activity. *Nutrients* **2019,** *11* (5).

25. Dellafiora, L.; Paolella, S.; Dall'Asta, C.; Dossena, A.; Cozzini, P.; Galaverna, G., Hybrid in silico/in vitro approach for the identification of angiotensin I converting enzyme inhibitory peptides from parma dry-cured ham. *J Agric Food Chem* **2015,** *63* (28), 6366-75.

26. Akif, M.; Masuyer, G.; Schwager, S. L.; Bhuyan, B. J.; Mugesh, G.; Isaac, R. E.; Sturrock, E. D.; Acharya, K. R., Structural characterization of angiotensin I-converting enzyme in complex with a selenium analogue of captopril. *FEBS J* **2011,** *278* (19), 3644-50.

27. Best, R. B.; Zhu, X.; Shim, J.; Lopes, P. E.; Mittal, J.; Feig, M.; Mackerell, A. D., Optimization of the additive CHARMM all-atom protein force field targeting improved sampling of the backbone φ, ψ and side-chain χ(1) and χ(2) dihedral angles. *J Chem Theory Comput* **2012,** *8* (9), 3257-3273.

28. Dellafiora, L.; Galaverna, G.; Cruciani, G.; Dall'Asta, C., A computational study toward the "personalized" activity of alternariol - Does it matter for safe food at individual level? *Food Chem Toxicol* **2019,** *130*, 199-206.

29. Aiello, G.; Li, Y.; Boschin, G.; Bollati, C.; Arnoldi, A.; Lammi, C., Chemical and biological characterization of spirulina protein hydrolysates: Focus on ACE and DPP-IV activities modulation. *J Funct Food*: 2019.

30. Aluko, R. E.; Girgih, A. T.; He, R.; Malomo, S.; Li, H.; Offengenden, M.; Wu, J. P., Structural and functional characterization of yellow field pea seed (*Pisum sativum* L.) protein-derived antihypertensive peptides. *Food Res Int* **2015,** *77*, 10-16.

31. Nongonierma, A. B.; Dellafiora, L.; Paolella, S.; Galaverna, G.; Cozzini, P.; FitzGerald, R. J., Approaches applied to the study of peptide analogs of Ile-Pro-Ile in relation to their dipeptidyl peptidase IV inhibitory properties. *Front Endocrinol (Lausanne)* **2018,** *9*, 329.

32. Martínez-Maqueda, D.; Miralles, B.; Recio, I.; Hernández-Ledesma, B., Antihypertensive peptides from food proteins: a review. *Food Funct* **2012,** *3* (4), 350-61.

33. Majumder, K.; Wu, J., Purification and characterisation of angiotensin I converting enzyme (ACE) inhibitory peptides derived from enzymatic hydrolysate of ovotransferrin. *Food Chem* **2011,** *126* (4), 1614-9.

34. Majumder, K.; Chakrabarti, S.; Morton, J. S.; Panahi, S.; Kaufman, S.; Davidge, S. T.; Wu, J. P., Egg-derived ACE-inhibitory peptides IQW and LKP reduce blood pressure in spontaneously hypertensive rats. *J Funct Foods* **2015,** *13*, 50-60.

35. Girgih, A. T.; He, R.; Aluko, R. E., Kinetics and molecular docking studies of the inhibitions of angiotensin converting enzyme and renin activities by hemp seed (*Cannabis sativa* L.) peptides. *J Agric Food Chem* **2014,** *62* (18), 4135-4144.

36. Mora, L.; Gallego, M.; Toldrá, F., ACEI-inhibitory peptides naturally generated in meat and meat products and their health relevance. *Nutrients* **2018,** *10* (9).

37. Fujita, H.; Yoshikawa, M., LKPNM: a prodrug-type ACE-inhibitory peptide derived from fish protein. *Immunopharmacology* **1999,** *44* (1-2), 123-7.

38. Nongonierma, A. B.; FitzGerald, R. J., Features of dipeptidyl peptidase IV (DPP-IV) inhibitory peptides from dietary proteins. *J Food Biochem* **2019,** *43* (1), 11.

39. Pak, V. V.; Koo, M. S.; Kasymova, T. D.; Kwon, D. Y., Isolation and identification of peptides from soy 11S-globulin with hypocholesterolemic activity. *Chem Nat Comp* **2005,** *41* (6), 710-714.

40. Pak, V. V.; Koo, M.; Kwon, D. Y.; Yun, L., Design of a highly potent inhibitory peptide acting as a competitive inhibitor of HMG-CoA reductase. *Amino Acids* **2012,** *43* (5), 2015-25.

Funding

This work was supported partially by Fondazione Cariplo, project “SUPER-HEMP: Sustainable Process for Enhanced Recovery of Hempseed Oil”, code number 2017-1005, and partially by the project ERA-NET SUSFOOD2: “DISCOVERY - Disaggregation of conventional vegetable press cakes by novel techniques to receive new products and to increase the yield”.

FIGURE CAPTIONS

Figure 1. Evaluation of the ACE inhibitory activity of P7 in renal HK-2 and intestinal Caco-2 cells. P7 reduces the ACE activity with a dose-response trend and IC_{50} of 79.6±0.20 μM and 13.7±0.28 μM, respectively. Data represent the mean±s.d. of three independent experiments performed in triplicate.

Figure 2. Transport of P7 across Caco-2 cells. Quantification of P7 in the BL compartment as a function of time: trend of P7 alone (green triangle) and in mixture (green dot). Data represent the mean±s.d. of three independent experiments performed in triplicate.

Figure 3. Incubation of LTFPG with DPP-IV and transport in Caco-2 monolayers. Incubation with DPP-IV: **(A)** TIC and EIC chromatograms of P7 and LTFPG, respectively; **(B)** tandem MS/MS spectrum of LTFPG; **(C)** peak intensity of LTFPG as a function of time of incubation with DPP-IV. Transport experiments in Caco-2 monolayers: **(D)** linear transport of LTFPG as a function of time.

Figure 4. Computational results of LTFPG. (A) Binding poses of LTFPG within the ACE catalytic sites and respective pharmacophoric analysis. The protein is represented in cartoon, while peptides and residues involved in polar interactions are represented in sticks. Zn ions are represented by spheres. Grey, red, and blue meshes indicate regions sterically and energetically favorable to receive hydrophobic, hydrogen bond acceptor, and hydrogen bond donor groups, respectively. Polar interactions are indicated by yellow dotted lines. The circles indicate the N-terminus of peptide. **(B)** RMSD analysis of LTFPG within the two catalytic sites of ACE. **(C)** Time-step representation of LPYP trajectories within the N- and C-domain of ACE. The from-red-to-blue color switch indicates the stepwise changes of ligand coordinates over time (50 nanosec). The yellow arrow indicates the movement of the N-terminus of LTFPG along the simulation.

Figure 5. **Investigation of LTFPG biological activities.** Effects of LTFPG on the in vitro DPP-IV **(A)** and HMGCoAR **(B)** activities, respectively. Data represent the mean±s.d. of three independent experiments performed in triplicate. C: control sample; (***) $p<0.001$

Table 1. Metabolites Produced at AP Side When P7 is Tested as Individual Species and Within a Mixture.

Peptide sequences	$[M+H]^+$	m/z	Mixture	Alone
LTFPGSAED (P7, parent peptide) [a]	936.43	469.80	X	X
TFPGSAED (AP metabolite)	823.20	823.20	X	-
LTFPG (AP metabolite) [a]	534.29	534.29	X	-

[a] P7 and LTFPG were test at 1 mg/mL, respectively

FIGURE GRAPHICS

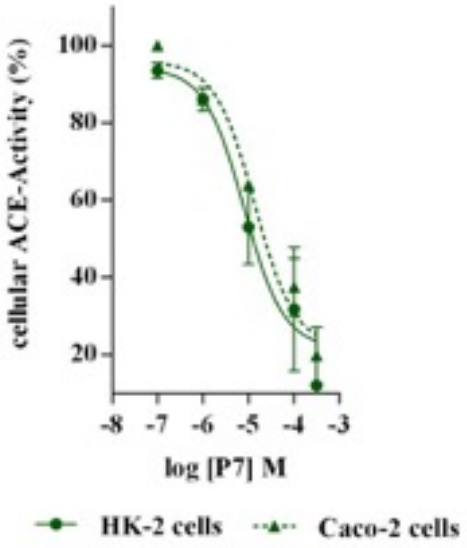

Figure 1

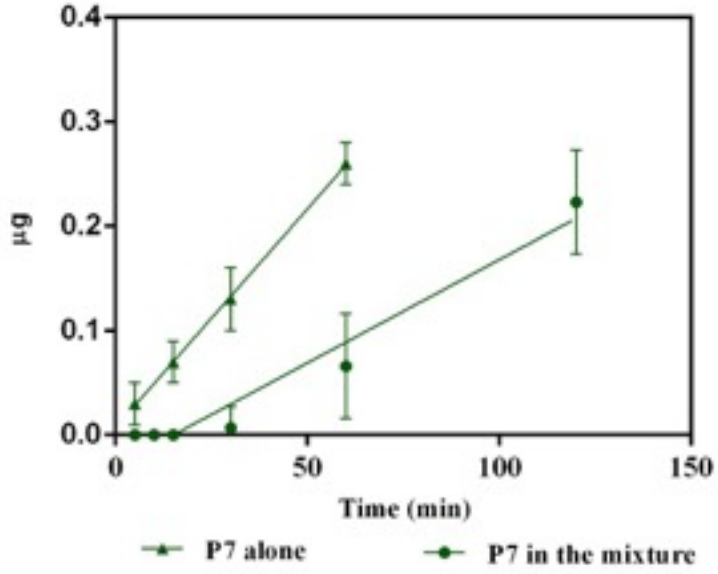

Figure 2

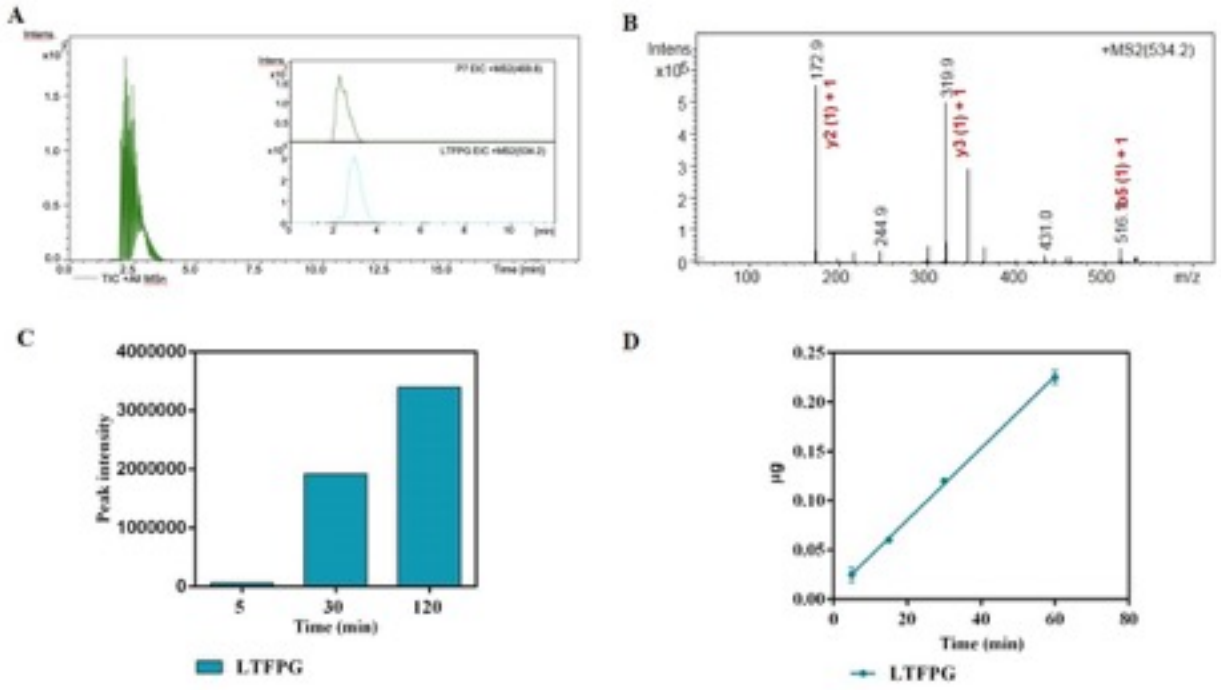
A
B
+MS2(534.2)
172.9
319.9
244.9
431.0
516.
y2 (1) + 1
y3 (1) + 1
100
200
300
400
500
m/z
C
Peak intensity
4000000
3000000
2000000
1000000
0
5
30
120
Time (min)
LTFPG
D
μg
0.25
0.20
0.15
0.10
0.05
0.00
0
20
40
60
80
Time (min)
LTFPG

Figure 3

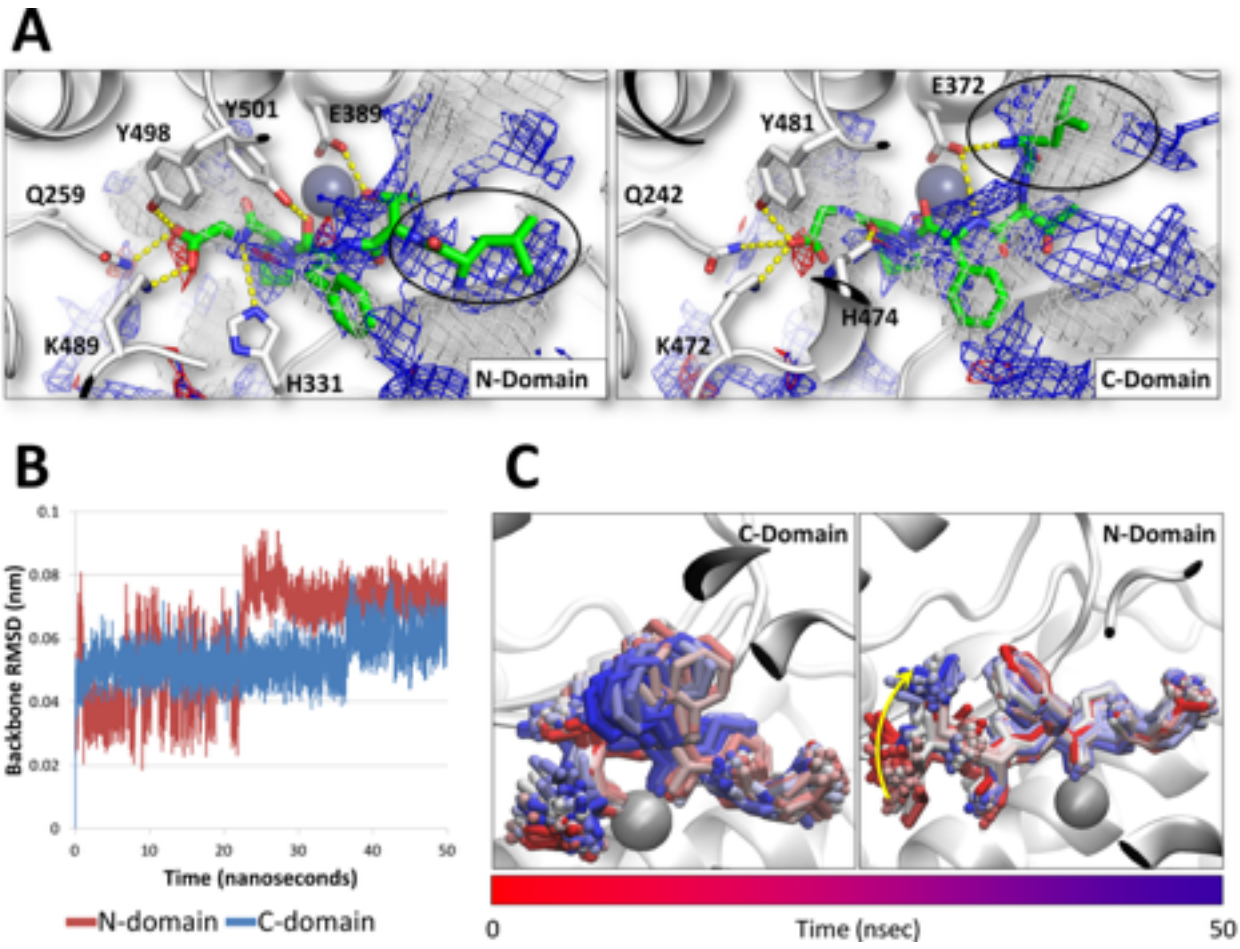
A
Y498
Y501
E389
Q259
K489
H331
N-Domain
E372
Y481
Q242
H474
K472
C-Domain
B
Backbone RMSD (nm)
0.1
0.08
0.06
0.04
0.02
0
0
10
20
30
40
50
Time (nanoseconds)
N-domain
C-domain
C
C-Domain
N-Domain
0
Time (nsec)
50

Figure 4

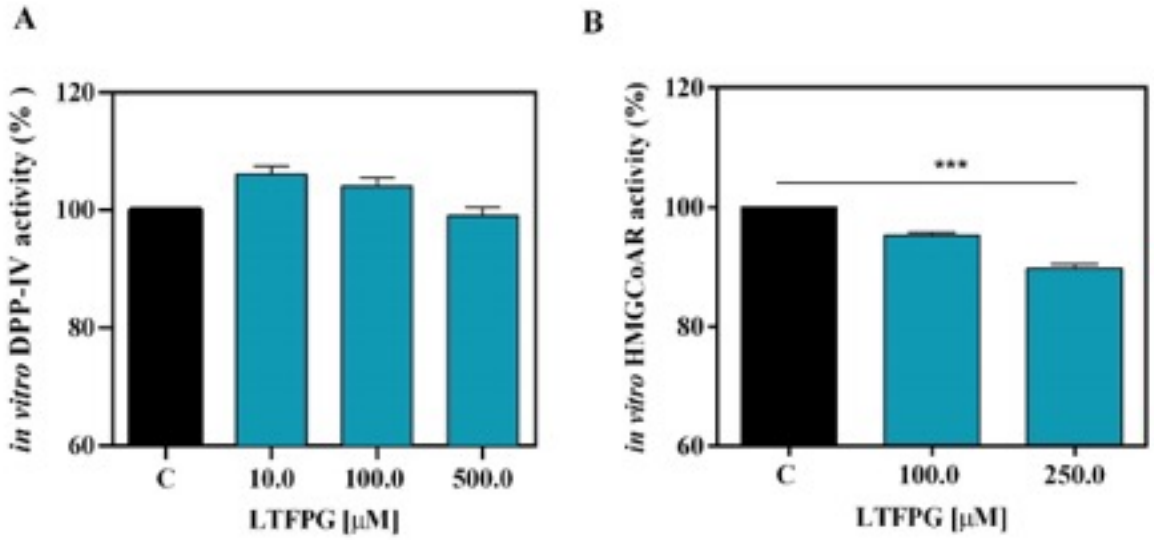
A
in vitro DPP-IV activity (%)
120
100
80
60
C
10.0
100.0
500.0
LTFPG [μM]
B
in vitro HMGCoAR activity (%)
120
100
80
60
***
C
100.0
250.0
LTFPG [μM]

Figure 5

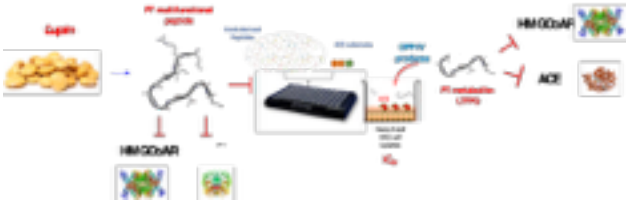

TOC